IEEE Access
Multidisciplinary | Rapid Review | Open Access Journal

Received July 8, 2021, accepted September 25, 2021, date of publication October 4, 2021, date of current version October 13, 2021.

Digital Object Identifier 10.1109/ACCESS.2021.3117922

Weak Magnetic Signal Characteristics for Critical Damage of Oil and Gas Pipelines Based on Electron Spinning

GUOQING WANG[1,2], LIUWEI MAO[1], AND DU DU[1]
[1]Naval Research Institute, Beijing 100071, China
[2]School of Information Science and Engineering, Shenyang University of Technology, Shenyang 110870, China

Corresponding author: Guoqing Wang (wangguoqing@sut.edu.cn)

This work was supported in part by the National Natural Science Foundation of China under Grant 61571308, and in part by Liaoning Province Natural Science Foundation of China under Grant 2019-MS-243.

ABSTRACT Stress and deformation are important factors that affect the safe operation of pipelines. Plastic deformation in the pipeline indicates a state of critical damage. Based on micro-magnetization and stress equivalent magnetic field theories, the change mechanism of ferromagnetic materials under external stress is analyzed. The 3D simulation model of the iron–carbon alloy system is established by the Material Studied software, and the relationship between the system magnetism and stress is obtained by calculating the electronic spin state distribution changes under different stress applications. The pipeline suppression experiment is designed to study the change characteristics of the magnetic induction intensity on the pipeline surface during the repeated suppressions until yield. Results show that the weak magnetic signal continuously varies as the pressure on the pipeline increases. The greater the pressure, the lower the magnetic induction intensity on the pipe surface. The pipeline exhibits different weak magnetic signal characteristics in the elastic and plastic deformation stages. The magnetic signal variation curve has apparent inflection points. The deformation and damage states of the pipeline can be assessed by the change characteristics of the weak magnetic signal. Repeated suppression causes the pipeline magnetism to weaken and the initial magnetization of the material to decrease. The experimental results are consistent with the theoretical analysis.

INDEX TERMS Critical damage, electron spinning, equivalent magnetic field, weak magnetic.

I. INTRODUCTION

Ferromagnetic pipelines are the main transportation mode of important energy and media in the world, and their applications cover various fields such as energy, equipment, and engineering production. At present, the total oil and gas pipeline built has exceeded 250×10^4km worldwide, and continues to increase every year [1]. Pipeline transportation of oil and gas has become an important industry related to national economic and social development. Due to its running characteristics and work environment, oil and gas pipelines have characteristics of high pressure, flammability, explosion, and corrosion, which determine the importance of its safety management. Pipeline operations have two high-risk periods. One is the pressure test and the trial operation stages during the construction and commissioning of newly built pipelines. Second, after the pipeline has been in service for a certain period of time, the pipe body gradually incurs defects such as corrosion, fatigue, and cracks. With the extension of the pipeline's service time, the external cyclic loads with pipeline aging and fatigue bring huge risks to its safe operations, and may even induce destruction [2]. Given that the materials have good plasticity and toughness, pipeline failure accidents are generally caused by yielding or plastic deformation in the body [3]. Therefore, such local plastic deformation indicates that the pipeline is on the verge of damage. If this plastic deformation is effectively detected, then the damage can be predicted and presents high significance for ensuring pipeline safety [4], [5].

Under operating pressure, the plastic deformation of the pipeline is caused by local stress concentration. Inversely, the plastic deformation can be determined by detecting the

The associate editor coordinating the review of this manuscript and approving it for publication was Shunfeng Cheng.

stress concentration. Magnetic memory testing can characterize the stress concentration degree of the ferromagnetic material by detecting the irreversible magnetic field change characteristics on the material surface after the stress application in the geomagnetic environment [6]–[9]. On the basis of magnetic memory, weak magnetic detection is proposed to assess the stress concentration degree by detecting the weak magnetic field signal distribution and variation characteristics on the pipeline surface under the non-excitation state (earth magnetic field environment) [10]–[13]. This method is an online detection technology for pipeline stress concentration [14]–[16]. It has the advantages of lower equipment weight and strong passage ability for pipeline detection compared to conventional detection techniques. Given that the mechanism of the magnetic effect of stress has not been clarified, the qualitative and quantitative relationship between stress and weak magnetic field signal has always been a hot research topic [17]–[20]. The generation mechanism of weak magnetic signal under stress has been examined from different perspectives, but still no unified theory can explain all the phenomena of stress-magnetic coupling [21]–[25]. Starting from the micro-magnetism theory of ferromagnetic materials, this study analyzes the mechanism of weak magnetic signal generated by stress and calculates their qualitative and quantitative relationship through simulation. The weak magnetic signal characteristics of pipeline under cyclic load are studied by the actual suppression experiment. The foundation of weak magnetic detection technology for early damage stage of oil and gas pipelines is established.

II. ANALYSIS OF WEAK MAGNETIC DETECTION MECHANISM

When subjected to external force, the local area of the metal crystal undergoes stress concentration, such as crack tip, inclusion interface, or near surface damage. When the external force is small, only elastic deformation occurs, that is, after the stress is removed, the atoms return to their original positions and the abnormal signal disappears. When the external force exceeds a certain limit, a dislocation may occur. According to dislocation multiplication theory, as the external force increases, the dislocations in the crystal greatly increases and moves to the surface along a certain direction. Then, the metal undergoes slip and plastic deformation.

The magnetic field of ferromagnetic material comes from magnetization, wherein the interaction between atoms causes the spontaneous lattice distortion and deformation of its magnetic domain. When the ferromagnetic material is magnetized by an external magnetic field, the domain structure and its corresponding spontaneous deformation change, which results in the magnetostrictive effect. Similarly, the ferromagnetic material has an inverse hysteresis effect. When the ferromagnetic material is deformed under stress, the internal domain structure changes, resulting in a magnetostrictive state, that is, the effect of stress is similar to that of an external magnetic field. Under external force, this magnetism is determined by the inverse magnetostriction and hysteresis effects.

According to equivalent field theory which is propose by Jiles, the effect of stress on the magnetization process of ferromagnetic materials can be expressed by an equivalent magnetic field [26], [27]. In its absence, the non-hysteresis magnetization energy E of ferromagnetic material can be expressed as:

$$E = \frac{3}{2}\sigma\lambda + TS \tag{1}$$

where λ is the magnetostrictive constant, σ is the stress, T is the temperature, and S is the entropy.

The stress equivalent magnetic field H_σ is derived from the energy to the magnetization M:

$$H_\sigma = \frac{1}{\mu_0}\frac{\mathrm{d}E}{\mathrm{d}M} = \frac{3}{2}\frac{\sigma}{\mu_0}\frac{\mathrm{d}\lambda}{\mathrm{d}M} \tag{2}$$

When the stress σ_0 and the magnetization direction θ form an angle, the stress σ for isotropic materials should be expressed as:

$$\sigma = \sigma_0\left(\cos^2\theta - \upsilon\sin^2\theta\right) \tag{3}$$

where υ is Poisson's ratio.

Then, Equation (2) becomes:

$$H_\sigma = \frac{3}{2}\frac{\sigma}{\mu_0}\left(\frac{\mathrm{d}\lambda}{\mathrm{d}M}\right)_\sigma = \frac{3}{2}\frac{\sigma_0}{\mu_0}\left(\frac{\mathrm{d}\lambda}{\mathrm{d}M}\right)_\sigma\left(\cos^2\theta - \upsilon\sin^2\theta\right) \tag{4}$$

For a ferromagnet, the magnetization effect caused by stress is equivalent to that by an equivalent magnetic field H_σ. Thus, the non-hysteresis magnetization Man of ferromagnetic material under stress is given by Langevin equation:

$$M_{\mathrm{an}}(\sigma) = M_{\mathrm{s}}\left[\coth\left(\frac{H_\sigma}{\mathrm{a}}\right) - \frac{\mathrm{a}}{H_\sigma}\right] \tag{5}$$

where $\mathrm{a} = k_B T/\mu_0 M$, M_{s} is the spontaneous magnetization.

If the magnetostrictive constant λ of the material is obtained by approximation, the relationship between stress and weak magnetic signal can be obtained using Equation (5).

When the external field intensity decreases to zero, the magnetic domain cannot return to its initial state, that is, a certain effect remains and the internal magnetization is not zero. This remainder results in a certain remanence, and thereby the hysteresis effect. The change of magnetization of ferromagnetic material caused by stress can be considered as magnetizing the material. When the external force is removed, the magnetic domain cannot completely return to its initial state due to the moving resistance of the inner wall of the ferromagnetic material. In addition, the hysteresis effect also exists, that is, the ferromagnetic material magnetization decreases but is not complete. A certain residual magnetic field forms a weak magnetic signal, which reflects the stress state of the material.

III. THEORETICAL CALCULATION METHOD OF STRESS WEAK MAGNETIC SIGNAL

According to the equivalent field theory, the study on the magnetism of ferromagnetic materials under stress can be carried out by analyzing its micro atomic state. When the material is subjected to external force, the atomic spacing in the crystal increases and the potential field of each atom has a strong binding effect on the electron. An electron that is close to an atom is mainly affected by its atomic field, and the effect of others can be regarded as a perturbation. Considering the internal electronic and free atom states, the microscopic particle state can be expressed by the energy functional of electron density:

$$\left[\frac{\hat{p}^2}{2m} + U(\vec{r})\right]\phi_i(\vec{r}) = \varepsilon_i\phi_i(\vec{r}) \tag{6}$$

The electron wave function $\varphi_i(\vec{r})$ in Equation (6) is expanded by Bloch function in K space:

$$\varphi_i(\vec{r}) = \sum_{j,\gamma} A_{j\gamma}(k)b_{j\gamma}(k,\vec{r}) \tag{7}$$

where $\{A_{j\gamma}\}$ is the linear combination coefficient and $b_{jr}(k,\vec{r})$ is the Bloch function. In k space, this function is represented by the linear combination of atomic orbits $\phi_j(\vec{r})$, which can be expanded by Fourier series as:

$$b_{jr}(k,\vec{r}) = \frac{1}{\sqrt{N}}\sum_n \exp(jk\cdot R_n)\phi_j(\vec{r}-\tau_\gamma - R_n) \tag{8}$$

where N is the number of lattices in the unit solid volume, j is the orbital, γ represents the different atoms in the unit crystal cell, τ_γ is the lattice vector of the γ atom of n cell, and R_n is the positive lattice vector.

The combination coefficient $\{A_{j\gamma}\}$ can be found by substituting Equation (7) into Equation (6) and changing the inner product with $b_{j'\delta}(k,\vec{r})$:

$$\sum_\gamma A_{j\gamma}\left\langle b_{jr}(k,\vec{r})\left|H\right|b_{j'\delta}(k,\vec{r})\right\rangle = E\sum_\gamma A_{j\gamma}\left\langle b_{jr}(k,\vec{r})\middle|b_{j'\delta}(k,\vec{r})\right\rangle \tag{9}$$

where H is the Hamiltonian of the system.

According to Equation (8), the Eigenequation can be obtained:

$$\left|H_{j\gamma,j'\delta}(k) - S_{j\gamma,j'\delta}(k)E\right| = 0 \tag{10}$$

Among them:

$$H_{j\gamma,j'\delta}(k) = \sum_n \exp(-jk\cdot R_n) \times \left\langle\phi_j(\vec{r}-\tau_\gamma)\left|H\right|\phi_{j'}(\vec{r}-\tau_\delta-R_n)\right\rangle \tag{11}$$

$$S_{j\gamma,j'\delta}(k) = \sum_n \exp(-jk\cdot R_n) \times \left\langle\phi_j(\vec{r}-\tau_\gamma)\middle|\phi_{j'}(\vec{r}-\tau_\delta-R_n)\right\rangle \tag{12}$$

In Equation (11), the Hamiltonian H is:

$$H = -\frac{\hbar^2}{2m_e}\vec{\nabla}_i^2 + \frac{e^2}{4\pi\varepsilon_0}\int\frac{\rho(\vec{r}')}{|\vec{r}-\vec{r}'|}d\vec{r}' + v(\vec{r}) + \frac{\delta E_{xc}[\rho(\vec{r})]}{\delta\rho(\vec{r})} \tag{13}$$

The linear combination coefficient can be obtained from Eigenequation (10), and then the wave function of the system can be obtained using Equation (7). Then, the electron spin density of states and energy band structure of the solid system can be calculated by substituting Equation (7) into Equation (6). The tight binding method has the advantage that the calculation is relatively small, but only considers the changes of the electronic states of the outer s-orbitals of atoms. For the study of the magnetomechanical effect of ferromagnetic crystals under external force, the electronic states of d-orbitals also need consideration. Thus, the error of the model calculation results is large.

IV. SIMULATION OF STRESS FIELD WEAKENING SIGNAL

The steel materials commonly used in pipelines are taken as the research object, and the software CASTEP is used based on solid energy band theory. The simulation calculation model with characteristics of iron carbon alloy is established. Figure 1 shows the model, a three-dimensional structure composed of several iron and carbon atoms, including a, b, and c crystal directions. This structure can simulate the three-dimensional stress state of actual pipeline material under internal pressure.

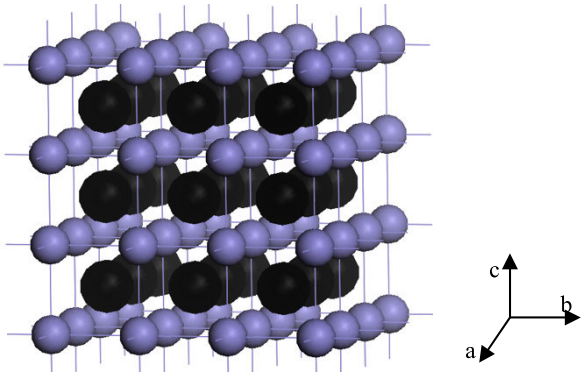

FIGURE 1. Three-dimensional simulation model.

The tight binding method is used in the model calculation. The sampling of K point in Brillouin zone is set as 16 × 16 × 16, and the cut-off energy is calculated as 300 ev. For the system exchange correlation in the theoretical model, the RPBE function (one of revision functions) in the generalized gradient approximation is used.

A. MODEL OPTIMIZATION

According to the law of thermodynamics, as the energy of the system decreases, the stability increases. In the preliminary structure model of ferromagnetic crystal, the energy of the system is not the lowest state, and direct calculation leads

to errors in the results. Therefore, energy optimization of the crystal is carried out to obtain the most stable crystal structure, and thereby accurately calculate the magnetic characteristics under external force.

The model optimization method is geometry optimization. In the model optimization, the energy of the system is continuously circulating and self-consistent, and finally converges to a lower amount to reach a stable equilibrium state and reach the optimum structure. Figure 2 shows the energy optimization of the model.

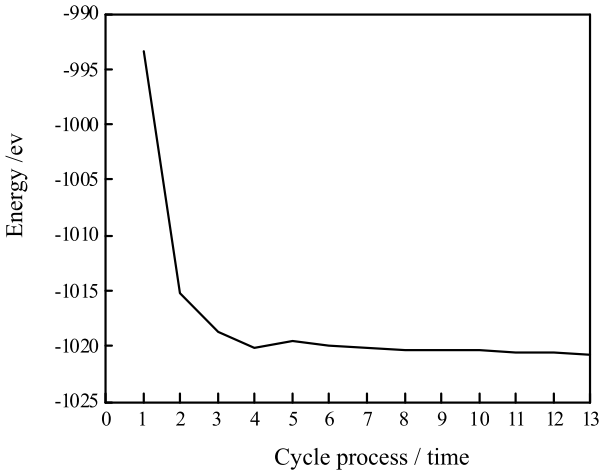

FIGURE 2. Model optimization curve.

As shown above, the energy of the ferromagnetic crystal system gradually decreases and reaches the minimum through multiple cycles. Then, the system finally reaches a stable state. This result indicates that the energy is optimized and the model crystal reaches the most stable state. On this basis, the magnetic properties of materials under stress can be quickly and accurately calculated.

B. MAGNETIC PROPERTIES OF GROUND STATE

The magnetism of ferromagnetic materials comes from atoms, and that of atoms comes from the state of electron spin. Ferromagnetic coupling is calculated to obtain the motion law and distribution characteristics of spin electrons under various external forces, including their density of states and atomic magnetic moment, and then to study the weak magnetic signal characteristics of the system under stress.

In ferromagnetic crystals, the atoms have several electrons whose spin states determine the magnetism. Spin electrons are distributed in the outer orbits. Less affected by the Coulomb effect of the nucleus, these orbital electrons therefore have spin exchanges with those of neighboring atoms. At the same time, the outer electrons of ferromagnetic materials also have exchange between orbits. Therefore, the orbital electrons of ferromagnetic crystals redistribute, changing the electron cloud configuration in and between the orbits and varies from those of individual atoms. The spin electrons in the outer parts of the system can travel between orbits and occupy varying energy states at different times, forming the electron cloud distribution state. These roving electron clouds are distributed in the energy band that is composed of several energy states, thus forming the system structure. By calculating the electron distribution, the motion characteristics of spin electrons can be obtained and the magnetic characteristics of the system can be analyzed.

Figure 3 shows the results of electronic density of states of ferromagnetic system in the ground state without external force. For the ferromagnetic system in the ground state, the electron spin density is concentrated near the Fermi level and the peak value of the density of states is large, indicating a strong ferromagnetism.

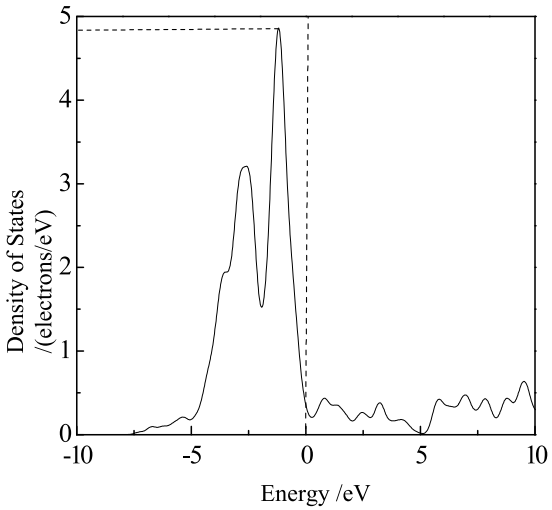

FIGURE 3. Ground state electron distribution of the system without external force.

C. CALCULATION OF ELECTRON DISTRIBUTION UNDER EXTERNAL FORCE

The actual pipe wall is subjected to three-dimensional stress under internal medium pressure, and thus stress in three directions of a, b, and c is applied to the established model in the simulation. By changing the applied force, the magnetic characteristics of the system under different stresses are simulated. According to microscopic magnetization theory of matter, the magnetism of ferromagnets comes from the movement and distribution of electrons, and their density of states in the system can be used to assess the magnetic characteristics. Through the simulation model, the electronic state change characteristics of the system under four different stresses of 5, 10, 15, and 20MPa are calculated. Figure 4 shows the results.

The simulation results show that the electron density of states of the system has strong ferromagnetism under low external force, and the electron distribution density is highest near the Fermi level with zero energy. With the increase of external force, the system still shows characteristics of ferromagnetic state but the electron distribution density near the Fermi level decreases, which indicates a

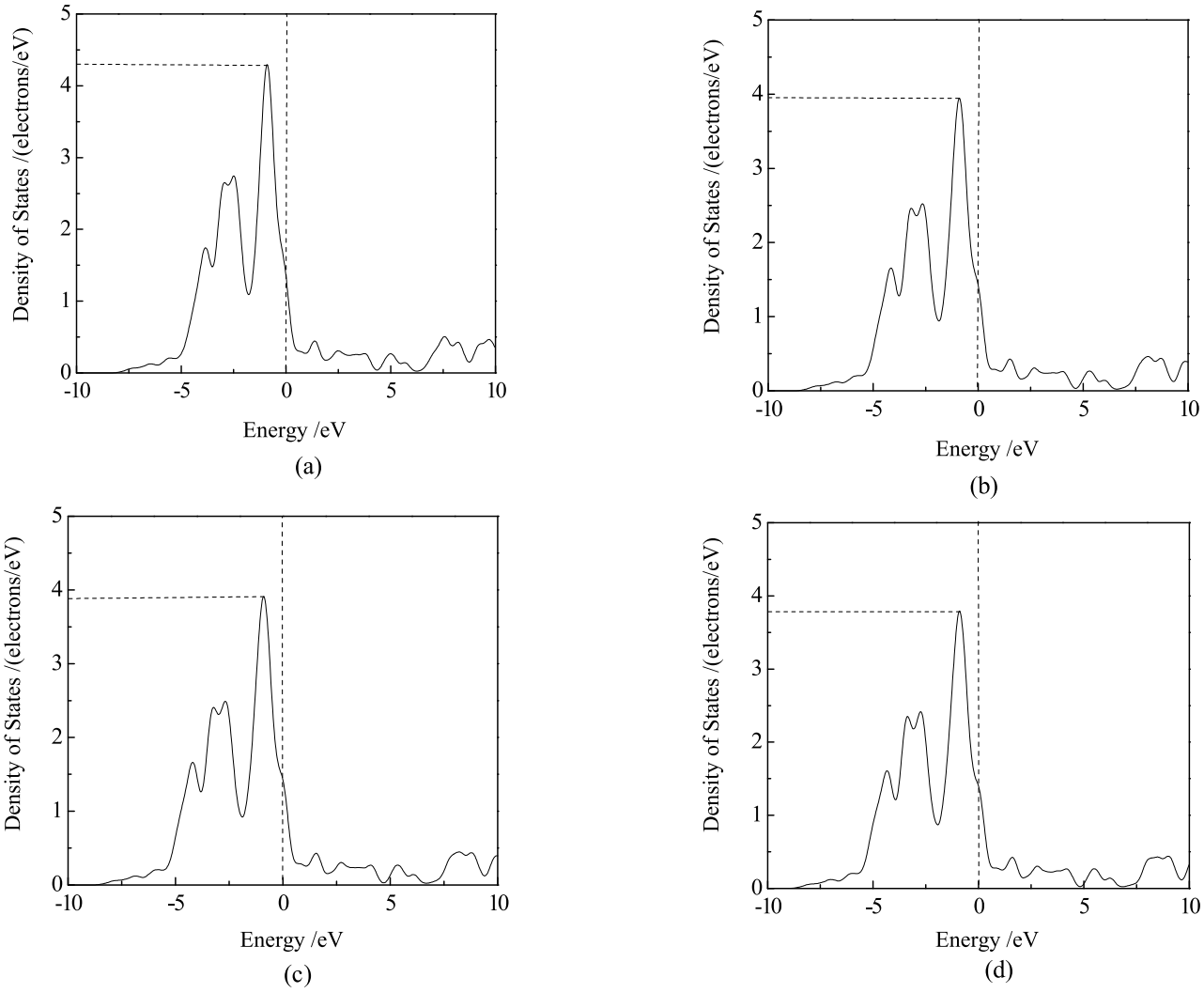

FIGURE 4. Electronic spin state distribution of the system under different stresses: (a) 5Mpa; (b)10MPa; (c)15Mpa; (d) 20MPa.

weakening magnetism. When the stress reaches 20MPa, the change of the electronic state slows down, which indicates changes in the internal atomic structure due to the generation of dislocations after the plastic deformation of the material, which hinders the interaction between atoms. The change of magnetic properties differs from that of elastic deformation.

D. ATOMIC MAGNETIC MOMENT

Calculating the electron spin density of states under pressure allows for the qualitative analysis of the influence of stress on the magnetic characteristics of ferromagnetic crystal. Thus, the variation law of the magnetic properties of the system is obtained. To intuitively reflect the abovementioned effect, we follow these steps: quantitatively analyze the influence of stress on the weak magnetic signal; clarify the weak magnetic effect of ferromagnetic materials under three-dimensional stress state; calculate the atomic magnetic moment of the system under each stress state; and obtain the influence of three-dimensional stress on the magnetic coupling relationship of ferromagnetic system and the weak magnetic effect. The magnetic characteristics of materials under repeated application of external force are compared by calculating the atomic magnetic moment of the system for each loading. Figure 5 shows the results corresponding to each stress.

Under the three-dimensional tensile stress state, the atomic magnetic moment of the system gradually decreases as the stress increases during the two loading applications. When the stress exceeds 15MPa, the change trend of the atomic magnetic moment of the system slows down, the slope of the curve decreases, and the change curve forms an inflection point. The results show that the weak magnetic signal characteristics of ferromagnetic system abruptly changes during the transition from elastic to plastic deformation under three-dimensional stress, and the magnetic characteristics of the ferromagnetic system change under plastic deformation. At the same time, when the external force is withdrawn (initial state of the second loading), the change of magnetic

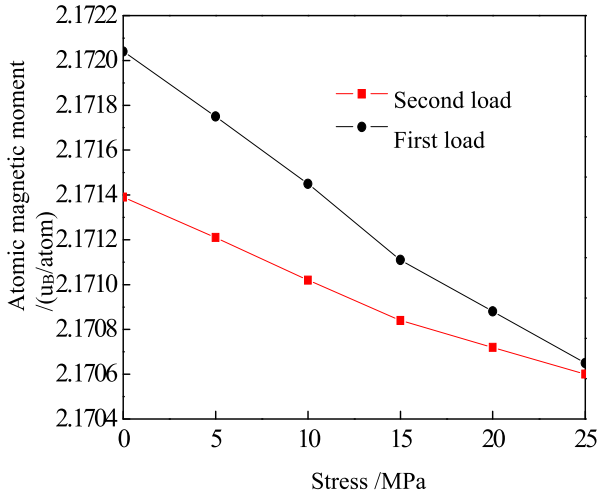

FIGURE 5. Atomic magnetic moments of two ferromagnetic systems under triaxial tensile stress.

properties of the ferromagnet are retained to a certain extent. After the plastic deformation, an irreversible magnetic change state is formed, which is reflected in the lower magnetic moment of the ferromagnetic material in the second loading than in the first loading. The slope of the relationship between the atomic magnetic moment and stress of the plastic deformation ferromagnetic system is smaller than that of the normal state, which indicates the weakened coupling degree of ferromagnetic material. The variation of atomic magnetic moment under stress is characterized by weak signals of the ferromagnetic material.

V. EXPERIMENTAL DETAILS

A. EXPERIMENTAL DESIGN

To eliminate the influence of the shape effect of the limited size test piece on the weak magnetic signal, a 100 m long experimental pipe was designed. The pipe material is X52 and the size is $\Phi 273 \times 6$ mm. To reflect the repeatability of the weak magnetic detection signal, we select two locations as the signal collection points in different directions of the experimental pipe section. Figure 6 shows the experimental design. The weak magnetic probe is a self-developed, high-sensitivity sensor based on a differential coil. The minimum resolution is 1nT. The probe is placed along the X (radial) and Y (axial)

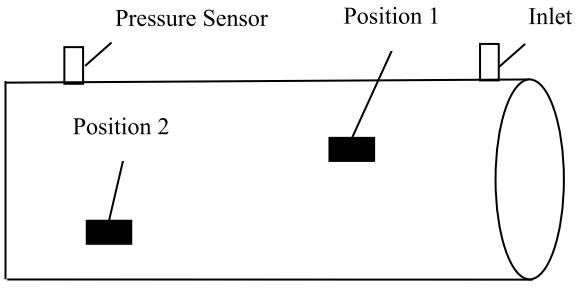

FIGURE 6. Schematic diagram of experimental design.

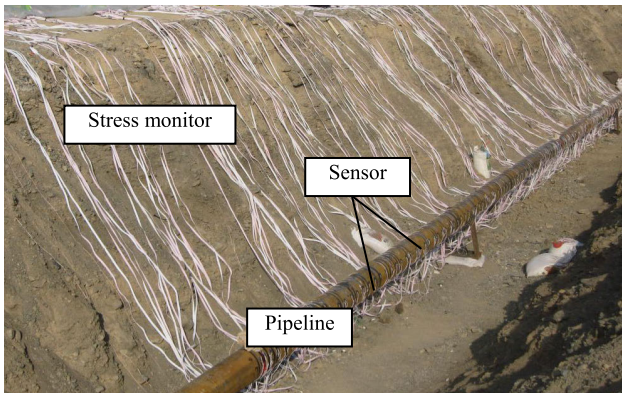

FIGURE 7. Experimental site diagram.

directions to collect the magnetic signals in the corresponding directions. Strain gauges are placed near the weak magnetic probe to monitor the deformation state of the pipe body. Figure 7 shows the fixed position of the weak magnetic probe and the experimental site.

The experimental method is to apply pressure to the pipeline. Through water injection and pressurization, the deformation of the pipe body and the characteristics of weak magnetic signal under different internal pressures are detected. Pressure is applied until the yield state and then the pressure is released to zero. Subsequently, the pressure is re-applied to detect the weak magnetic signal characteristics of the pipeline in the yield state and the repeated yielding. The experiment includes eight cycles of pressure application. The weak magnetic probe is fixed at position 1 in the first to fourth pressure application, and at position 2 in the fifth to eighth pressure application. Table 1 shows the maximum pressure corresponding to each application.

TABLE 1. Number of applied and maximum pressure.

Sequence	1	2	3	4	5	6	7	8
Maximum pressure/MPa	14.377	15.200	15.430	15.728	15.876	16.080	16.239	16.750

B. EXPERIMENTAL RESULTS AND ANALYSIS

Figure 8 shows the stress and strain monitoring results of positions 1 and 2 during the pressure applications.

In the eight cycles, the strain of the pipeline increases linearly as the pressure increases. When the pressure reaches the yield point of the pipe, the rate of change of the pipe strain varies. The curve shows an inflection point, where the plastic deformation begins. At this moment, the eight applications of pressure on the pipe reach the yield point. The monitoring results show that as the number of pressure applications increases, the yield stress of the pipe also increases, indicating that the internal dislocation increases and the material continues to harden.

Figures 9 and 10 show the detection results of the pressure-magnetic signal changes during the pressure application.

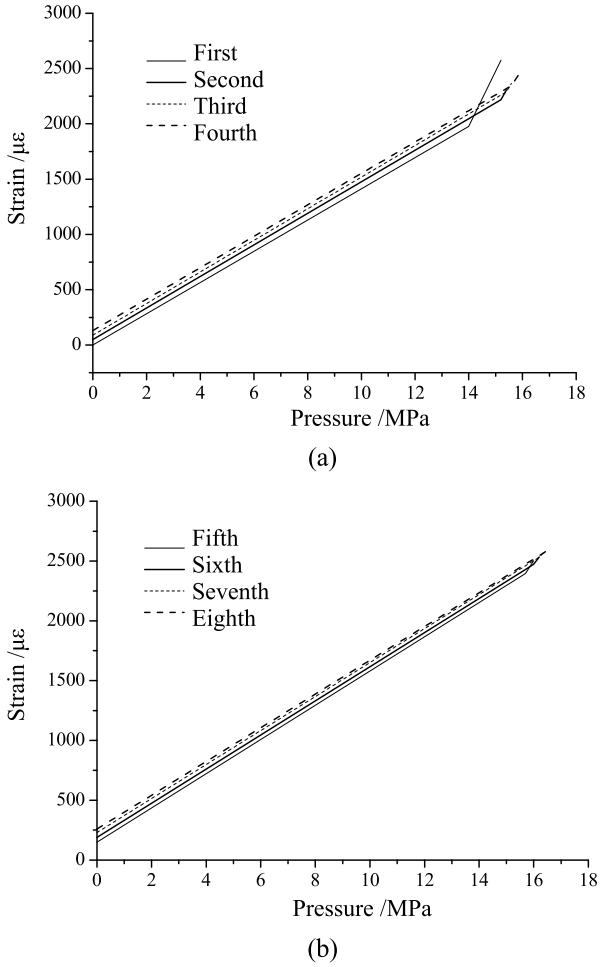

FIGURE 8. Strain monitoring results during pressure application: (a) Position 1 Pressure strain curve; (b) Position 2 Pressure strain curve.

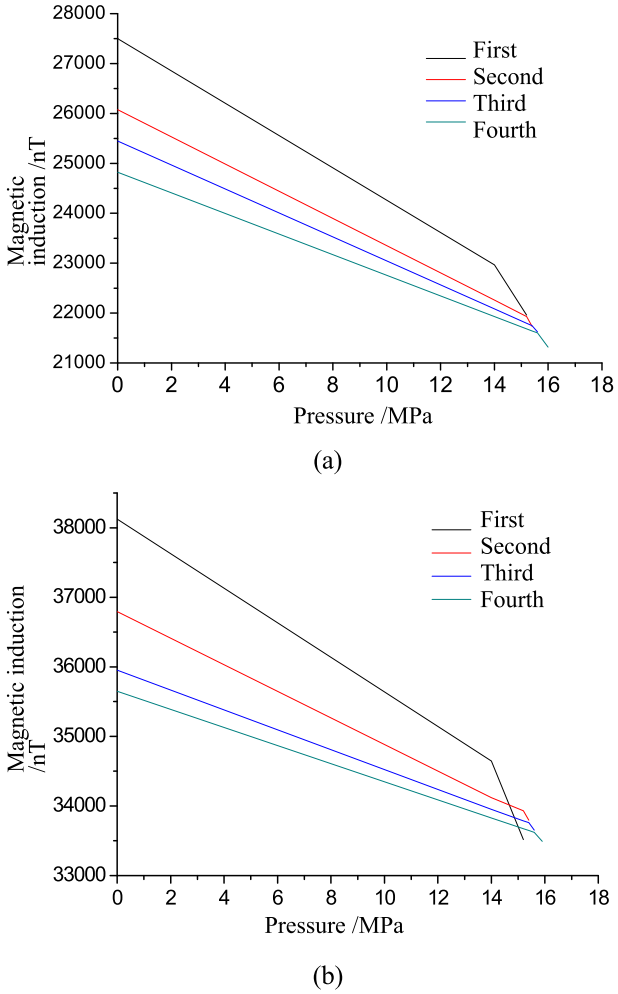

FIGURE 9. Position 1 pressure-magnetic signal relationship curve: (a) X-direction magnetic signal and pressure (1–4 times); (b)Y-direction magnetic signal and pressure (1–4 times).

Figure 9 shows that as the applied pressure increases, the weak magnetic field signals in the X and Y directions of position 1 gradually decrease, magnetic induction intensity gradually decreases, and the magnetism of the material weakens. The pipeline reaches yield point when the magnetic field signal changes slowly. The pressure–magnetic signal relationship curve has a change point, indicating that the material has different changing speeds during the elastic and plastic deformation stages. The curve can be used to determine the position of material yielding. The change point corresponds to the yield point of the pipe, and continues to move to the right as the number of pressure applications increases, appearing at a greater pressure point. In addition, the initial value of the magnetic induction intensity of the pipe surface gradually decreases each time the pressure is applied. After the pressure is applied, the change in the magnetic field is not completely removed and a remanence is observed.

Figure 10 shows that in applying pressure, the X-direction magnetic field at position 2 decreases as the pressure increases, and the magnetic induction intensity continues to decrease. When the pipe reaches the yield point, the magnetic signal slowly changes. The plastic deformation stage also shows a different magnetic induction intensity change from that of the elastic deformation stage, and the curve shows the change points of different deformation stages. Because of the inverse measurement direction, the initial value of the Y-direction magnetic field at position 2 is negative. As the pressure increases, the absolute value of the magnetic induction intensity decreases, and the magnetism also gradually weakens. When the pipe reaches the yield point, the change speed of the magnetic signal also becomes slow and the magnetic induction intensity shows a change characteristic different from the elastic deformation stage. As the number of pressure applications increases, the change point continues to move toward greater pressure. At the same time, the test results show that the initial change of the magnetic field before each suppression has the same characteristics as the realization of the X-direction magnetic field, which also reflects a certain remanence.

The detection results of Figures 9 and 10 show that during plastic deformation under stress, the weak magnetic field signal characteristics of the pipe surface changes, and can thereby serve as a basis for assessing pipeline damage.

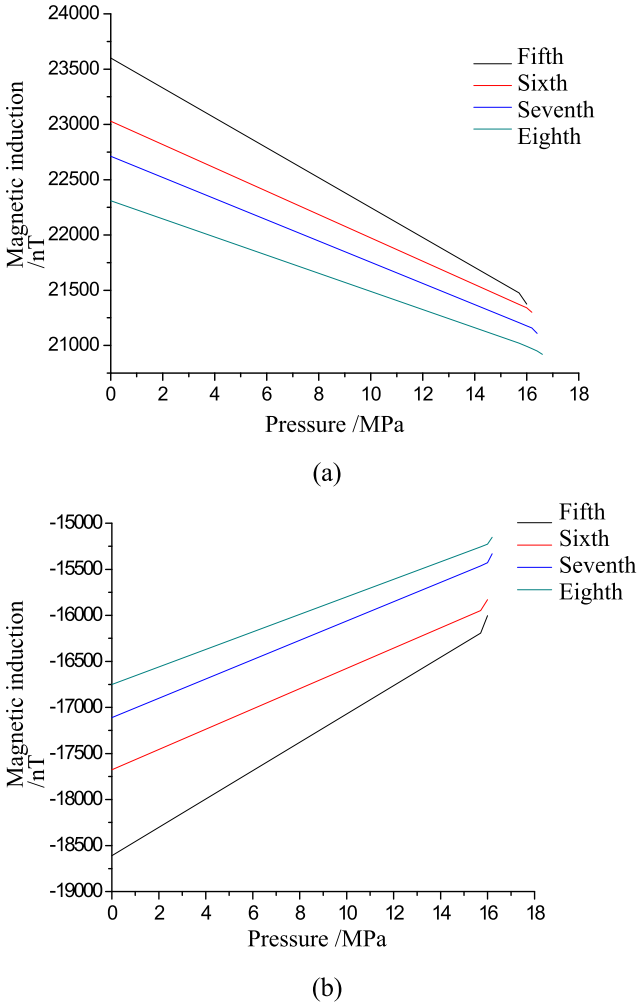

FIGURE 10. Position 2 pressure-magnetic signal relationship curve: (a) X-direction magnetic signal and pressure (5–8 times); (b) Y-direction magnetic signal and pressure (5–8 times).

VI. CONCLUSION

(1) Under external force, ferromagnetic materials produce changes in the electron interaction of the microscopic system, leading to changes in its magnetic properties. The increase in pressure causes the magnetic properties of the system to weaken. In different deformation stages, the magnetic properties have different change characteristics.

(2) During the stress and deformation of the pipeline, the weak magnetic signal on the surface of the pipe body changes accordingly, showing a change in the size of the weak magnetic field. As pressure increases, the magnetic induction intensity of the pipe body surface decreases, and behaves so during the elastic and plastic deformation stages. According to different speeds, the varying deformation states of the pipe can be assessed by the changing points of the magnetic signal curve.

(3) Through detection of the weak magnetic field of the pipeline, plastic deformation and its impending damage state can be predicted. Thus, the critical state of the pipeline can be identified and analyzed based on repeatedly loading and measurement.

REFERENCES

[1] Q. Z. Zhu, P. X. Duan, J. H. Wang, Q. Y. Li, C. X. Zhan, N. Shi, and Y. P. Zhang, "Current situations and future development of oil and gas pipelines in the world," *Oil Gas Storage Transp.*, vol. 34, no. 12, pp. 1262–1266, Dec. 2015.

[2] G. Q. Wang, L. J. Yang, and B. Liu, "Study on the testing method of oil-gas pipeline stress damage based on magnetic memory," *Chin. J. Sci. Instrum.*, vol. 38, no. 2, pp. 271–278, Feb. 2017.

[3] W. Z. Yan, J. Z. Zhang, Z. G. Zhou, and Z. F. Yue, "Study on the indentation behaviors of bicrystals based on crystal plasticity theory," *Acta Metallurgica Sinica*, vol. 51, no. 1, pp. 100–106, Jan. 2015.

[4] H. Huang, C. Yang, Z. Qian, G. Han, and Z. Liu, "Magnetic memory signals variation induced by applied magnetic field and static tensile stress in ferromagnetic steel," *J. Magn. Magn. Mater.*, vol. 416, pp. 213–219, Oct. 2016, doi: 10.1016/j.jmmm.2016.04.094.

[5] G. Wang, L. Yang, P. Yan, and L. Wei, "Test procedure for stress damage of ferromagnetic materials based on metal magnetic memory effects," *Mater. Test.*, vol. 60, no. 3, pp. 301–305, Mar. 2018, doi: 10.3139/120.111151.

[6] L. Sun, X. Liu, and H. Niu, "A method for identifying geometrical defects and stress concentration zones in MMM technique," *NDT E Int.*, vol. 107, Oct. 2019, Art. no. 102133, doi: 10.1016/j.ndteint.2019.102133.

[7] A. Dubov, A. Dubov, and S. Kolokolnikov, "Application of the metal magnetic memory method for detection of defects at the initial stage of their development for prevention of failures of power engineering welded steel structures and steam turbine parts," *Weld. World*, vol. 58, no. 2, pp. 225–236, Mar. 2014, doi: 10.1007/s40194-013-0102-y.

[8] A. Dubov and S. Kolokolnikov, "The metal magnetic memory method application for online monitoring of damage development in steel pipes and welded joints specimens," *Weld. World*, vol. 57, no. 1, pp. 123–136, Feb. 2013, doi: 10.1007/s40194-012-0011-5.

[9] A. Dubov and S. Kolokolnikov, "Assessment of the material state of oil and gas pipelines based on the metal magnetic memory method," *Weld. World*, vol. 56, nos. 3–4, pp. 11–19, Mar. 2012, doi: 10.1007/BF03321331.

[10] C. Pang, J. Zhou, Q. Zhao, R. Zhao, Z. Chen, and Y. Zhou, "A new method for internal force detection of steel bars covered by concrete based on the metal magnetic memory effect," *Metals*, vol. 9, no. 6, p. 661, Jun. 2019, doi: 10.3390/met9060661.

[11] L. J. Yang, G. Q. Wang, and S. W. Gao, "The study on force magnetic coupling signal character of magnetic memory based on OPWP algorithm," *Chin. J. Sci. Instrum.*, vol. 37, no. 7, pp. 1588–1595, Jul. 2016.

[12] M. X. Xu, Z. H. Chen, and M. Q. Xu, "Mechanism of magnetic memory signal variation in the process of fatigue," *J. Mech. Eng.*, vol. 50, no. 4, pp. 53–59, Apr. 2014, doi: 10.3901/JME.2014.04.053.

[13] J. Leng, Y. Liu, G. Zhou, and Y. Gao, "Metal magnetic memory signal response to plastic deformation of low carbon steel," *NDT E Int.*, vol. 55, pp. 42–46, Apr. 2013, doi: 10.1016/j.ndteint.2013.01.005.

[14] L. J. Li and X. G. Zhang, "Discrimination method of wire rope fault signal based on Holzer sensor for multi array weak magnetic detection," *Cluster Comput.*, vol. 22, no. 2, pp. 901–906, Mar. 2019, doi: 10.1007/s10586-018-2440-4.

[15] M. Konowalczyk, O. F. V. Elst, and J. G. Storey, "Development of lock-in based overtone modulated MARY spectroscopy for detection of weak magnetic field effects," *Phys. Chem. Chem. Phys.*, vol. 23, no. 2, pp. 1273–1284, Jan. 2021, doi: 10.1039/d0cp04814c.

[16] S. Bao, M. Fu, Z. Zhao, and P. Jin, "Quantitative stress evaluation and defect identification in ferromagnetic steels based on residual magnetic field measurements," *Mater. Eval.*, vol. 79, no. 3, pp. 311–319, Mar. 2021, doi: 10.32548/2021.me-04186.

[17] S. M. Kolokolnikov, A. A. Dubov, and A. Y. Marchenkov, "Determination of mechanical properties of metal of welded joints by strength parameters in the stress concentration zones detected by the metal magnetic memory method," *Weld. World*, vol. 58, no. 5, pp. 699–706, Sep. 2014, doi: 10.1007/s40194-014-0151-x.

[18] S. C. Chikr, A. Kaci, and A. A. Bousahla, "A novel four-unknown integral model for buckling response of FG sandwich plates resting on elastic foundations under various boundary conditions using Galerkin's approach," *Geomech. Eng.*, vol. 21, no. 5, pp. 471–487, Jun. 2020, doi: 10.12989/gae.2020.21.5.471.

[19] M. Augustyniak and Z. Usarek, "Discussion of derivability of local residual stress level from magnetic stray field measurement," *J. Nondestruct. Eval.*, vol. 34, no. 3, pp. 1–9, 2015, doi: 10.1007/s10921-015-0292-x.
[20] S. Kim, K. Kim, K. Choe, U. JuHyok, and H. Rim, "A nonlinear magneto-mechanical coupling model for magnetization and magnetostriction of ferromagnetic materials," *AIP Adv.*, vol. 10, no. 8, Aug. 2020, Art. no. 085304, doi: 10.1063/5.0016489.
[21] S. Bao, M. Fu, H. Lou, and S. Bai, "Defect identification in ferromagnetic steel based on residual magnetic field measurements," *J. Magn. Magn. Mater.*, vol. 441, pp. 590–597, Nov. 2017, doi: 10.1016/j.jmmm.2017.06.056.
[22] S. Bao, H. Lou, and Z. Zhao, "Evaluation of stress concentration degree of ferromagnetic steels based on residual magnetic field measurements," *J. Civil Struct. Health Monitor.*, vol. 10, no. 1, pp. 109–117, Feb. 2020, doi: 10.1007/s13349-019-00372-5.
[23] Y. Ege, S. Bicakcá, H. Gunes, H. Citak, and M. Coramik, "An application of BRANN and MFL methods: Determining crack type and physical properties on m5 steel sheets," *Measurement*, vol. 138, pp. 545–556, May 2019, doi: 10.1016/j.measurement.2019.02.064.
[24] Z. Qu, H. Wang, Y. Ding, W. Wang, and Y. Zheng, "Nondestructive detection and analysis of skidding damage for bearing steel 100Cr6 using improved magnetic Barkhausen noise technique," *J. Nondestruct. Eval.*, vol. 38, no. 4, pp. 1–11, Dec. 2019, doi: 10.1007/s10921-019-0634-1.
[25] B. Liu, H. Zhang, L. He, J. Ren, and L. Yang, "Quantitative study on the triaxial characteristics of weak magnetic stress internal detection signals of pipelines based on the theory of magnetoelectric coupling," *Measurement*, vol. 177, Jun. 2021, Art. no. 109302, doi: 10.1016/j.measurement.2021.109302.
[26] H. Hauser, Y. Melikhov, and D. C. Jiles, "Examination of the equivalence of ferromagnetic hysteresis models describing the dependence of magnetization on magnetic field and stress," *IEEE Trans. Magn.*, vol. 45, no. 4, pp. 1940–1949, Apr. 2009, doi: 10.1109/TMAG.2008.2009877.
[27] D. C. Jiles, "Theory of the magnetomechanical effect," *J. Phys. D, Appl. Phys.*, vol. 28, no. 8, pp. 1537–1546, 1995.

GUOQING WANG was born in Liaoning, China, in 1980. He received the B.S. and M.S. degrees in mechanical engineering from Liaoning Shihua University, Fushun, China, in 2003 and 2009, respectively, and the Ph.D. degree in information engineering from Shenyang University of Technology, Shenyang, China, in 2017.

From 2017 to 2018, he has been an Assistant Professor with the Department of Information Science and Engineering, Shenyang University of Technology. Since 2019, he has been a Postdoctoral Researcher with Naval Research Institute. He is the author of five books, more than 30 articles, and more than eight inventions. His research interests include materials testing, stress detection technology and related theory, and nondestructive testing technology. He is also a member of the Electromagnetic Professional Committee of the Chinese Society of Mechanical Engineering.

LIUWEI MAO was born in Shanxi, China, in 1985. He received the Ph.D. degree in ship and marine engineering from Naval University of Engineering, Wuhan, China, in 2015. Since 2015, he has been an Engineer with Naval Research Institute. His research interest includes ship structural mechanics.

DU DU received the Ph.D. degree in ship and marine engineering from Naval University of Engineering, Wuhan, China, in 2003. Since 2003, he has been a Senior Engineer with Naval Research Institute. His research interests include design and manufacture of ships and marine structures and ship general technology.